

# A comparative study on heat dissipation, morphological and magnetic properties of hyperthermia suitable nanoparticles prepared by co-precipitation and hydrothermal methods

MD SHARIFUL ISLAM, YOSHIHUMI KUSUMOTO\*, JUNICHI KURAWAKI,  
MD ABDULLA-AL-MAMUN and HIROTAKA MANAKA†

Department of Chemistry and Bioscience, Graduate School of Science and Engineering, Kagoshima University,  
1-21-35 Korimoto, Kagoshima 890-0065, Japan

†Department of Electrical and Electronics Engineering, Graduate School of Science and Engineering,  
Kagoshima University, 1-21-35 Korimoto, Kagoshima 890-0065, Japan

MS received 5 December 2011; revised 14 April 2012

**Abstract.** Magnetite ( $\text{Fe}_3\text{O}_4$ ) nanoparticles were prepared by co-precipitation and hydrothermal methods and their phase transfer was done successfully to compare their performances in different aspects. Synthesized nanoparticles were characterized for XRD, FE-SEM, TEM, UV-Vis absorption (reflectance) spectra, magnetic hysteresis loops and a.c. magnetic field induced hyperthermia. The magnetic nanoparticles prepared by the co-precipitation method show superior performances in respect of heat dissipation capability, saturation of magnetization values and particle size when compared to those prepared by the hydrothermal method.

**Keywords.** Heat dissipation; hyperthermia; hysteresis loops; reproducibility; magnetic nanoparticles.

## 1. Introduction

The synthesis of nanostructured magnetic materials has become a particularly important area of research and is attracting a growing interest because of the potential applications such materials have in ferrofluids, advanced magnetic materials, catalysts, coloured pigments, high-density magnetic recording media and medical diagnostics (Caruso *et al* 2001; Hyeon *et al* 2001; Yu *et al* 2002; Xiong *et al* 2003; Woo *et al* 2003; Wang *et al* 2003). Magnetic iron oxide nanoparticles and their dispersions in various media have long been of scientific and technological interest. Iron oxides exist in many forms in nature, with magnetite ( $\text{Fe}_3\text{O}_4$ ), maghemite ( $\gamma\text{-Fe}_2\text{O}_3$ ) and hematite ( $\alpha\text{-Fe}_2\text{O}_3$ ) which are probably most common (Cornell and Schwertmann 2003). Magnetite ( $\text{Fe}_3\text{O}_4$ ) has recently been considered an ideal candidate for biological applications, both as a tag for sensing and imaging, and as an activity agent for antitumor therapy (Häfeli *et al* 1997; Louie *et al* 2000; Perez *et al* 2004). Magnetite and maghemite have attracted attention in biomedical applications because of their biocompatibility and low toxicity in the human body (Tartaj *et al* 2005; Kim *et al* 2006). Magnetite and hematite have been used as catalysts for a number of industrially important reactions (Bautista *et al* 2007; Shi *et al* 2007; Li *et al* 2008), including the synthesis of  $\text{NH}_3$  (the Haber process), the high

temperature water gas shift reaction and the desulfurization of natural gas. The therapeutic potential of nanoparticles with a controlled and adapted size has been demonstrated in cases, where hyperthermia has been recognized as a promising therapy to treat tumorous areas (Bertorelle *et al* 2003; Perrin-Cocon *et al* 2003).

Superparamagnetic nanoparticles when exposed to an alternating magnetic field can be used to heat tumor cells to 41–45 °C, where tissue damage for normal tissue is reversible while the tumor cells are irreversibly damaged (Neuberger *et al* 2005). Under hydrothermal conditions, a broad range of nanostructured materials can be formed; this strategy is based on a general phase transfer and separation mechanism occurring at the interfaces of the liquid, solid and solution phases present during synthesis. In the co-precipitation method, size, shape and composition of the magnetic nanoparticles strongly depend on the type of salts used (e.g. chlorides, sulfates, nitrates), the  $\text{Fe}^{2+}/\text{Fe}^{3+}$  ratio, the reaction temperature, the pH value and ionic strength of the media (Lu *et al* 2007). While a number of suitable methods have been developed for the synthesis of magnetic nanoparticles (MNPs) of various different compositions, successful application of such magnetic nanoparticles in the areas listed above is highly dependent on the stability of the particles under a range of different conditions. Although hydrothermal and co-precipitation methods are based on the wet chemical synthesis, there are some significant differences in synthesized MNPs followed by both methods and they are also discussed for comparison in our study to find out their hyperthermia potentiality.

\* Author for correspondence (kusumoto@sci.kagoshima-u.ac.jp)

## 2. Experimental

### 2.1 Materials and methods

Typical syntheses of magnetic nanoparticles (MNPs) were carried out in a hydrothermal system by modified reduction reactions between  $\text{FeCl}_2$  and ethylene glycol and the reaction between  $\text{Fe}^{2+}$  and  $\text{Fe}^{3+}$  in a co-precipitation method (Hong *et al* 2005; Anselm 2008). In this experiment, chemicals used for synthesis of MNPs by both methods were iron chloride hexahydrate ( $\text{FeCl}_3 \cdot 6\text{H}_2\text{O}$ ), ethylene glycol (99.5%),  $\text{FeCl}_3$ , HCl, 25%  $\text{NH}_3$  solution (Wako Pure Chemical Industries Ltd., Japan),  $\text{FeCl}_2$  (Strem Chemicals, Newburyport), polyethylene glycol 4000 (Tokyo Kasei Kogyo Co. Ltd, Japan) and anhydrous sodium acetate (NaAc, 98%, Nacalai Tesque, Japan). All chemicals were of analytical grade and used without any further purification.

### 2.2 Hydrothermal synthesis of magnetic nanoparticles (MNPs)

$\text{FeCl}_3 \cdot 6\text{H}_2\text{O}$  (1.352 g, 5 mmol) was dissolved in ethylene glycol (40 mL) to form a clear solution, followed by the addition of NaAc (3.6 g) and polyethylene glycol (1.0 g). The mixture was stirred vigorously for 45 min until getting a clear solution and then sealed in a teflonlined stainless-steel autoclave (50 mL capacity). The autoclave was heated to and maintained at 200 °C for 5 h and allowed to cool to room temperature. After cooling, decantation was done by a permanent magnet to get the sedimented black products. The black products were washed several times with ethanol and dried at 70 °C for 3 h. Finally, we obtained  $\text{Fe}_3\text{O}_4$  nanoparticles.

### 2.3 Synthesis of MNPs by co-precipitation method

In a typical co-precipitation method,  $\text{FeCl}_3$  (2.6 g) and  $\text{FeCl}_2$  (1.3 g) were dissolved in nitrogen gas ( $\text{N}_2$ ) purged 2.0 M hydrochloric acid solution and magnetically stirred under a continuous flow of  $\text{N}_2$ . The mixture was heated at 70 °C for 30 min and then the mixture was again heated for another 5 min under a blanket of  $\text{N}_2$ . Ammonia was added drop by drop to precipitate the magnetic nanoparticles and the black product formed was treated hydrothermally at 70 °C for 30 min. All aqueous solutions and suspensions were made using nanopure water (18 M $\Omega$  cm resistances). The resulting nanoparticles were subsequently separated from the reaction media under magnetic field and washed three times with nanopure water before drying. Finally the MNPs were oven dried at 70 °C for 3 h to get  $\text{Fe}_3\text{O}_4$ .

### 2.4 Phase transfer of $\text{Fe}_3\text{O}_4$ to $\gamma\text{-Fe}_2\text{O}_3$ and $\alpha\text{-Fe}_2\text{O}_3$

It is well known that  $\text{Fe}_3\text{O}_4$  can be oxidized to  $\gamma\text{-Fe}_2\text{O}_3$ , which can be further transformed into  $\alpha\text{-Fe}_2\text{O}_3$  at higher temperature (Bate 1975). However, magnetite ( $\text{Fe}_3\text{O}_4$ ) is not

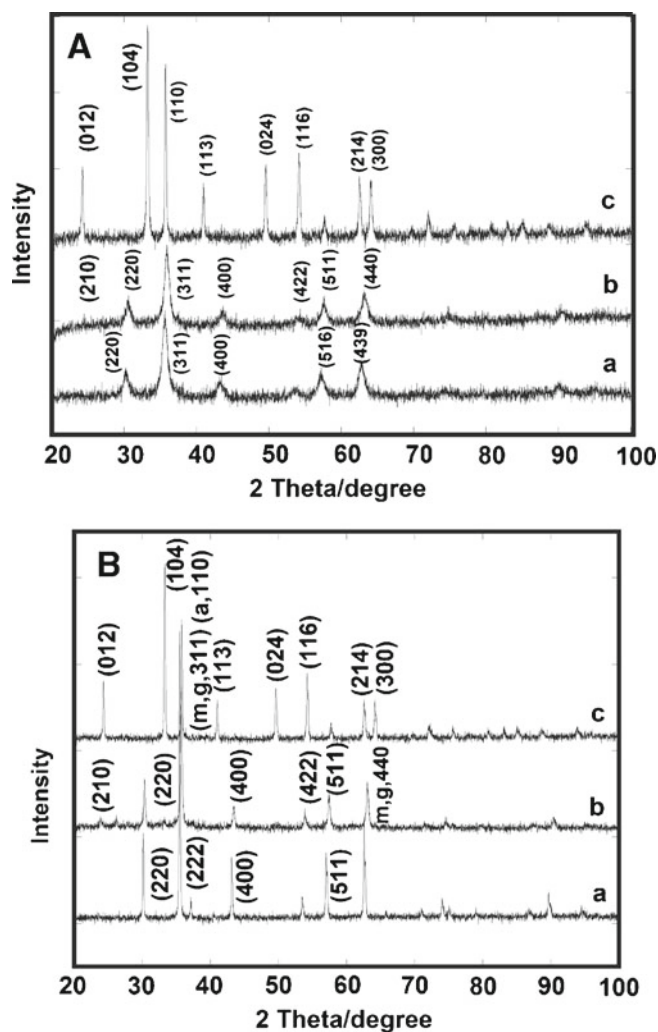


**Figure 1.** XRD patterns of MNPs synthesized by (A) co-precipitation and (B) hydrothermal methods. Magnetite, maghemite and hematite are represented by (a), (b) and (c), respectively in both plates (A) and (B).

very stable and is sensitive to oxidation. Magnetite is transformed into maghemite ( $\gamma\text{-Fe}_2\text{O}_3$ ) in the presence of oxygen (Laurent *et al* 2008). In figures 1A and B, (a) is the XRD pattern of the as-synthesized black  $\text{Fe}_3\text{O}_4$  nanoparticles assembly by both methods. After oxidation at 250 °C for 6 h, the black assembly is transformed into a red-brown one. Image (b) for both plates of figure 1 shows all XRD peak positions and relative intensities of this red-brown material, whereas image (c) shows XRD of the dark red-brown materials,  $\alpha\text{-Fe}_2\text{O}_3$ , obtained after 500 °C annealing of  $\gamma\text{-Fe}_2\text{O}_3$  in figure 1A(b) and B (b) under Ar gas for 1 h. However, the as-synthesized  $\text{Fe}_3\text{O}_4$  nanoparticles do not go through such a change if annealed under inert atmosphere. Even at 650 °C,  $\text{Fe}_3\text{O}_4$  structure is still retained, as evidenced by both XRD and TEM (data not shown). This confirms that the valence state of the iron cations in the as-synthesized sample closely matches with that of  $\text{Fe}_3\text{O}_4$  rather than similarly structured  $\gamma\text{-Fe}_2\text{O}_3$  (Sun *et al* 2004).

### 3. Structure and magnetic characterization

The structural characterization including size and crystal structure of the as-synthesized magnetic nanoparticles by both methods was performed for all the samples without any size sorting. To further confirm the crystal structure and overall phase purity, nanoparticles with different sizes were examined using a PANalytical Advance X-ray diffractometer (XRD) with  $\text{CuK}\alpha$  radiation and a Ni filter. The surface morphology and nanoparticles size were determined using a field emission scanning electron microscope (FE-SEM, Hitachi S-4100H). Absorption spectra were recorded on UV-Vis absorption (reflectance) spectrophotometer (Shimadzu Corporation, UV-2450, Japan). The samples were standardized with barium sulphate coated glass substrate and its spectrum was used as the baseline. The spectra of all samples were measured in a wavelength range between 240 and 850 nm. AC magnetic field induced heating capability of magnetic nanoparticles was examined to observe the hyperthermia potentiality of  $\text{Fe}_3\text{O}_4$  and  $\gamma\text{-Fe}_2\text{O}_3$  (for both methods) by dispersing the nanoparticles in distilled water as well as a minimum essential medium (MEM) and magnetic hysteresis loops were measured by a superconducting quantum interference device (SQUID, Quantum Design MPMS-5). Further, shapes of the nanoparticles were analysed by transmission electron microscopy (TEM) using a JEOL JEM-3010 VII TEM operating at 300 kV.

### 4. Reproducibility of magnetic ( $\text{Fe}_3\text{O}_4$ , $\gamma\text{-Fe}_2\text{O}_3$ and $\alpha\text{-Fe}_2\text{O}_3$ ) nanoparticles

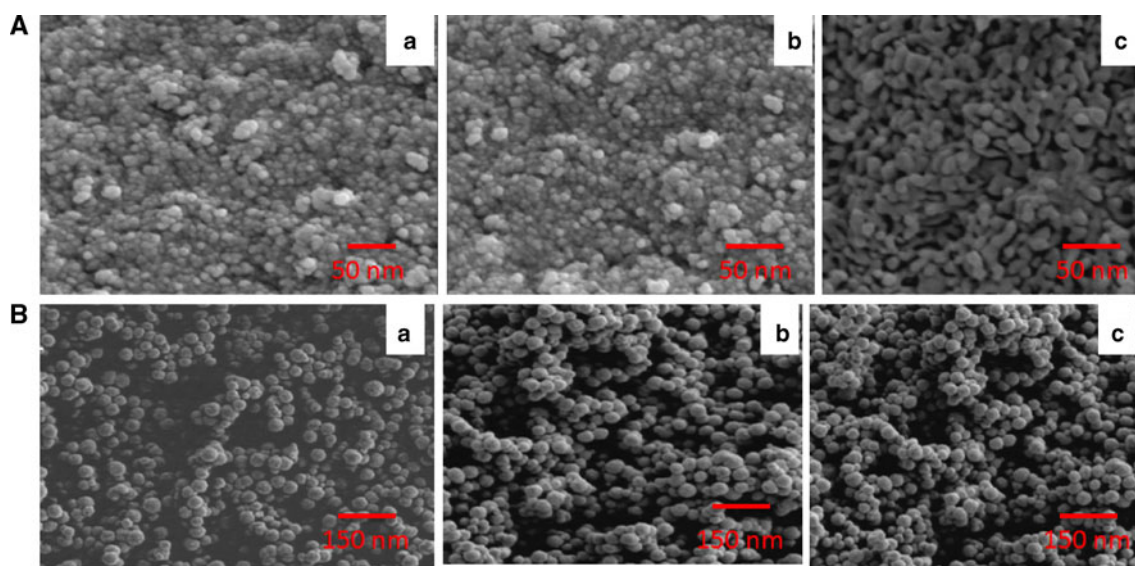
An important aspect of the synthesis of magnetic nanomaterials is the reproducibility when they are synthesized using

identical conditions. To test the reproducibility of magnetic nanoparticles, three samples were synthesized under optimum conditions already described in §§ 2.2, 2.3 and 2.4. All the characterizations of these samples were performed in accordance with § 3 and these three samples were found to have fairly consistent values for maximum reproducing capability. These results show excellent reproducibility for the synthesized magnetic nanoparticles by simple hydrothermal and co-precipitation methods which may be the key point for commercial production.

### 5. Results and discussion

The crystal structures of the prepared MNPs were observed by XRD measurement. Typical XRD patterns of  $\text{Fe}_3\text{O}_4$ ,  $\gamma\text{-Fe}_2\text{O}_3$  and  $\alpha\text{-Fe}_2\text{O}_3$  are shown in figure 1. As shown in figure 1, all samples were found to be consistent with the expected diffraction pattern of the *fcc* FeO structures for both methods. No diffraction peaks from other crystalline forms are detected, demonstrating that these  $\text{Fe}_3\text{O}_4$ ,  $\gamma\text{-Fe}_2\text{O}_3$  and  $\alpha\text{-Fe}_2\text{O}_3$  samples have high purity and crystallinity. Figure 1A demonstrated the peak indexes of (a)  $\text{Fe}_3\text{O}_4$ , (b)  $\gamma\text{-Fe}_2\text{O}_3$  and (c)  $\alpha\text{-Fe}_2\text{O}_3$  synthesized by co-precipitation method whereas the peak indexes of (a)  $\text{Fe}_3\text{O}_4$ , (b)  $\gamma\text{-Fe}_2\text{O}_3$  and (c)  $\alpha\text{-Fe}_2\text{O}_3$  synthesized by hydrothermal method is shown in figure 1B. More sharp narrower peaks were noticed among all the iron oxides prepared by hydrothermal method due to the larger particle size of  $\sim 45\text{--}50$  nm. In contrast, wide and broader peaks were noticed among all the iron oxides prepared by co-precipitation method due to the smaller particle size of  $\sim 15\text{--}20$  nm.

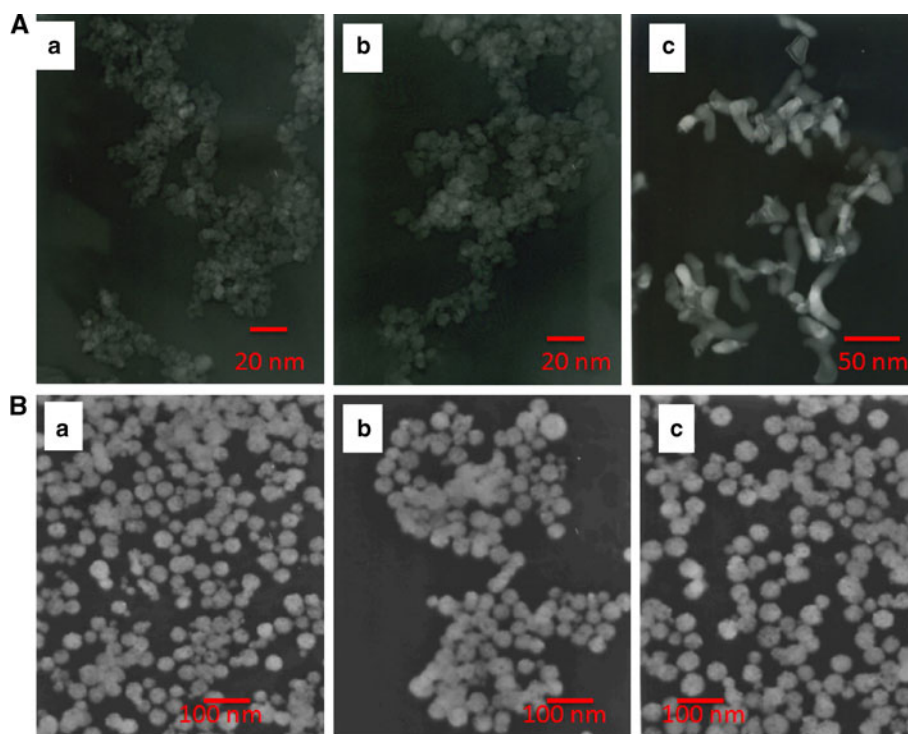
Particles morphology of all the samples was studied using FE-SEM (figure 2). Figures 2A and B represent FE-SEM



**Figure 2.** Comparative SEM images of magnetite, maghemite and hematite nanoparticles represented by (a), (b) and (c), respectively. Plate (A) for co-precipitation and (B) for hydrothermal method.

**Table 1.** Comparative performance of MNPs prepared by co-precipitation and hydrothermal methods.

| Property   | Co-precipitation                            |   |  | Hydrothermal                                |   |  |
|--|---|---|--|---|---|--|
|  | Magnetite<br>Fe <sub>3</sub> O <sub>4</sub> | Maghemite<br>γ-Fe <sub>2</sub> O <sub>3</sub> | Hematite<br>α-Fe <sub>2</sub> O <sub>3</sub> | Magnetite<br>Fe <sub>3</sub> O <sub>4</sub> | Maghemite<br>γ-Fe <sub>2</sub> O <sub>3</sub> | Hematite<br>α-Fe <sub>2</sub> O <sub>3</sub> |
| Particle size (SEM)  | 15–20 nm                                    | 15–20 nm                                      | 20–25 nm                                     | 45–50 nm                                    | 45–55 nm                                      | 50–60 nm                                     |
| Particle size (TEM)  | 12–18 nm                                    | 14–20 nm                                      | 25–35 nm                                     | 35–50 nm                                    | 40–55 nm                                      | 50–70 nm                                     |
| Particle shape   | Spherical                                   | Spherical                                     | Neck structured                              | Spherical                                   | Spherical                                     | Spherical                                    |
| Absorption edge  | 620 nm                                      | 600 nm  | 565 nm                                       | 650 nm                                      | 630 nm  | 570 nm                                       |
| Saturation value of magnetization ( <i>M<sub>s</sub></i> ) | 78 emu/g                                    | 59 emu/g                                      | 1.8 emu/g                                    | 65 emu/g                                    | 57 emu/g                                      | 1.2 emu/g                                    |

**Figure 3.** Comparative TEM images of magnetite, maghemite and hematite nanoparticles represented by (a), (b) and (c), respectively. Plate (A) for co-precipitation and (B) for hydrothermal method.

micrographs of (a) Fe<sub>3</sub>O<sub>4</sub>, (b) γ-Fe<sub>2</sub>O<sub>3</sub> and (c) α-Fe<sub>2</sub>O<sub>3</sub> synthesized by co-precipitation and hydrothermal methods, respectively. The nanoparticles size was roughly estimated to be about 15–20 nm and 45–55 nm prepared by co-precipitation and hydrothermal methods, respectively. This result revealed that co-precipitation method facilitates smaller size nanoparticles than hydrothermal method (table 1).

The samples were also characterized using TEM (figure 3) to analyse shape and size of the particles. Here figures 3A and B depict TEM micrographs of (a) Fe<sub>3</sub>O<sub>4</sub>, (b) γ-Fe<sub>2</sub>O<sub>3</sub> and (c) α-Fe<sub>2</sub>O<sub>3</sub> synthesized by co-precipitation and hydrothermal methods, respectively. Spherical-shaped morphology was observed by FE-SEM in (a) Fe<sub>3</sub>O<sub>4</sub> and (b) γ-Fe<sub>2</sub>O<sub>3</sub> but neck-structured in (c) α-Fe<sub>2</sub>O<sub>3</sub> (figure 2A)

for co-precipitation method whereas all spherical-shaped morphology was found in (a) Fe<sub>3</sub>O<sub>4</sub>, (b) γ-Fe<sub>2</sub>O<sub>3</sub> and (c) α-Fe<sub>2</sub>O<sub>3</sub> synthesized by hydrothermal method (figure 2B). TEM images also clearly support FE-SEM data in terms of morphological and nanostructural analysis with particle size ~12–25 nm and 35–55 nm synthesized by co-precipitation and hydrothermal method, respectively (table 1).

Figure 4 gives UV-Vis absorption (reflectance) spectra of the synthesized magnetic nanoparticles by both methods. As shown in figure 4, absorption spectra of (a) Fe<sub>3</sub>O<sub>4</sub>, (b) γ-Fe<sub>2</sub>O<sub>3</sub> and (c) α-Fe<sub>2</sub>O<sub>3</sub> represents co-precipitation method whereas (d) Fe<sub>3</sub>O<sub>4</sub>, (e) γ-Fe<sub>2</sub>O<sub>3</sub> and (f) α-Fe<sub>2</sub>O<sub>3</sub> represent the absorption spectra of MNPs synthesized by hydrothermal method. It can be seen that the absorption edges of co-precipitation synthesized MNPs are more red-shifted than

those of MNPs synthesized by the hydrothermal method (table 1).

With the increase of calcination temperature (500 °C), absorption edge of the sample has some blue shift. The blue shift is presumably ascribed to the formation of the homogeneous Fe<sub>2</sub>O<sub>3</sub> nanoparticles for both methods. The bandgap energy of Fe<sub>2</sub>O<sub>3</sub> is 2.2 eV and can be activated by the light below 563 nm (Karunakaran and Senthilvelan 2006).

To further explore the low temperature magnetic properties of Fe<sub>3</sub>O<sub>4</sub> samples from both methods,  $M$ - $T$  curves in zero field cooling (ZFC) and field cooling (FC) processes with a 1 kOe applied field were measured, as shown in figure 5. For the co-precipitation sample, ZFC magnetization ( $M_s$ ) value was 9.8 emu/g (a) whereas for the hydrothermal Fe<sub>3</sub>O<sub>4</sub> sample, the ZFC magnetization ( $M_s$ ) value was

7.8 emu/g (b), but no peak was observed for both samples by both methods.

The comparative hysteresis curves obtained at room temperature (figure 6) show that the saturation value of magnetization ( $M_s$ ) of MNPs was prepared by both methods. Figures 6(A) and (B) represent  $M_s$  value of (a) Fe<sub>3</sub>O<sub>4</sub> 78, 59 emu/g and (b)  $\gamma$ -Fe<sub>2</sub>O<sub>3</sub> 65, 57 emu/g, respectively prepared by co-precipitation and hydrothermal methods. Moreover, figure 6(C) shows  $M_s$  value of  $\alpha$ -Fe<sub>2</sub>O<sub>3</sub> nanoparticles prepared by (a) co-precipitation and (b) hydrothermal methods (1.8 and 1.2 emu/g, respectively). Thus the results revealed that  $M_s$  values of all samples prepared by co-precipitation method were always higher than that of MNPs prepared by the hydrothermal method (table 1).

The  $M_s$  values for substances treated with oxygen and annealed are different from the mother sample for both cases. The difference in magnetization of both oxidized and non-oxidized samples indicates that the oxidation of magnetite into maghemite was completed and that maghemite was reduced at high temperature to hematite during annealing which was also supported by an XDR analysis.

Heat dissipation of magnetite and maghemite nanoparticles prepared by both methods was evaluated by using an a.c. magnetic field generator using maximum magnetic field intensity and a frequency of 5.0 kA/m and 560 Hz, respectively. The heat generated from samples was evaluated by exposing 5 mg/mL magnetic particle suspension dispersed in distilled water and then their different doses like 0.2, 0.4, 0.6, 0.8 and 1.0 mL/5 mL MEM under an a.c. magnetic field for about 10 min exposure time. The comparative temperature rise of the as-prepared magnetic nanoparticles suspensions against the exposure time is shown in figure 7. The highest temperatures achieved by Fe<sub>3</sub>O<sub>4</sub> and  $\gamma$ -Fe<sub>2</sub>O<sub>3</sub> nanoparticles were 49.9, 50.2 °C and 49.2 and 49.7 °C prepared by co-precipitation and hydrothermal methods, respectively. Thus the findings revealed that the highest temperature was achieved by all the samples prepared by co-precipitation method, whereas temperature of the hydrothermally prepared sample increased gradually against time and heat dissipated was well below that of co-precipitation samples

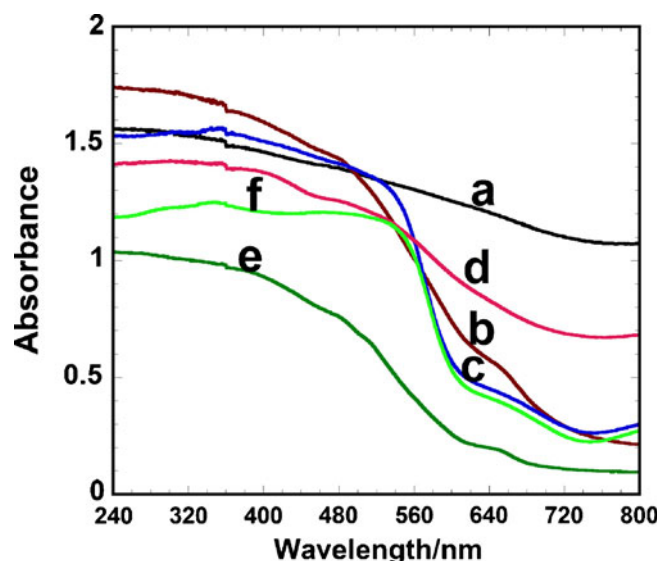


**Figure 4.** UV-Vis absorption (reflectance) spectra of MNPs. Magnetite, maghemite and hematite are represented by (a), (b), (c) and (d), (e), (f) for the co-precipitation and hydrothermal methods, respectively.

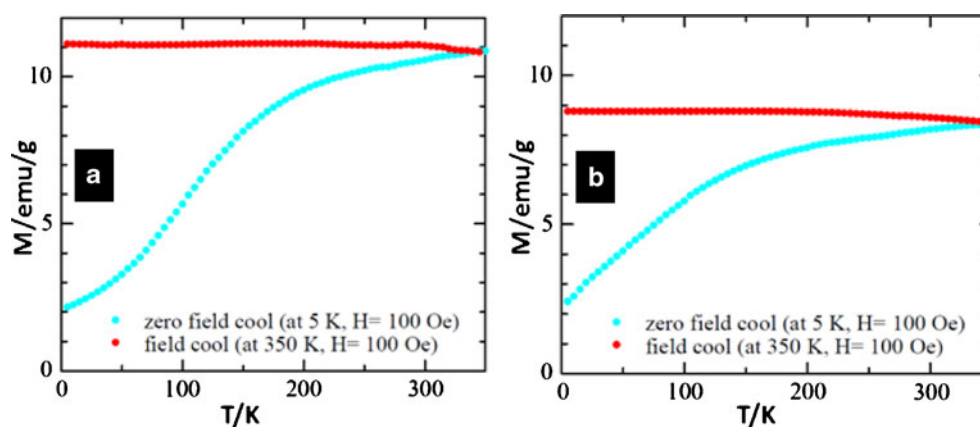


**Figure 5.** Temperature dependent magnetization in ZFC and FC processes for Fe<sub>3</sub>O<sub>4</sub> synthesized by co-precipitation (a) and hydrothermal (b) methods.

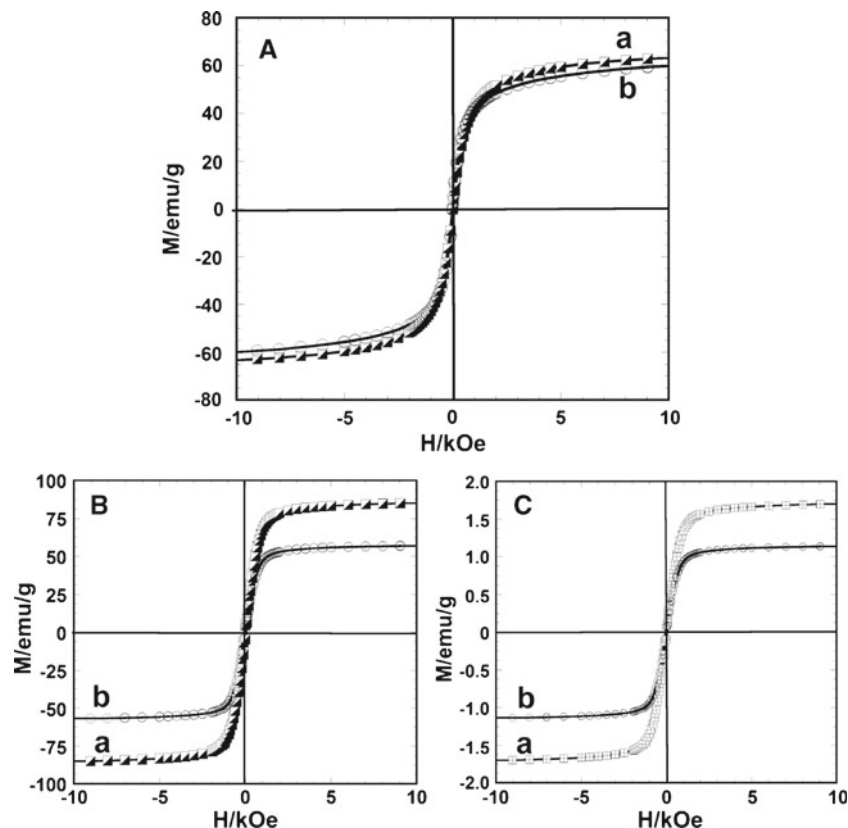


**Figure 6.** Comparative magnetic hysteresis loops of magnetic nanoparticles by co-precipitation and hydrothermal methods. Here  $M_s$  values of (a)  $\text{Fe}_3\text{O}_4$  and (b)  $\gamma\text{-Fe}_2\text{O}_3$  prepared by co-precipitation and hydrothermal methods are shown by (A) and (B), respectively whereas,  $M_s$  value of (C)  $\alpha\text{-Fe}_2\text{O}_3$  nanoparticles is prepared by (a) co-precipitation and (b) hydrothermal methods.

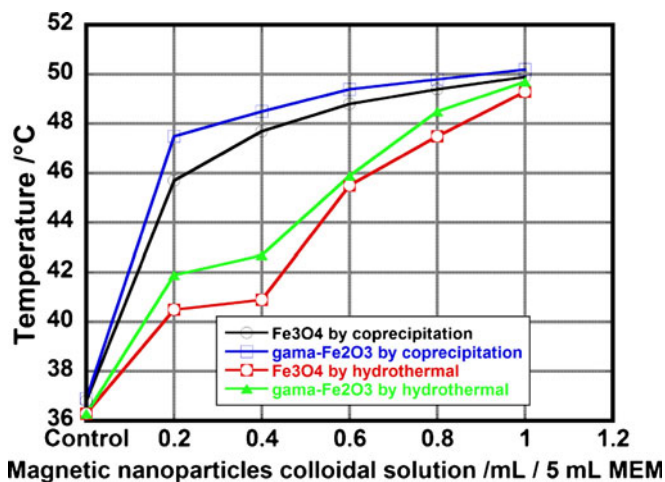


**Figure 7.** Comparative heat dissipation capability of MNPs by co-precipitation and hydrothermal methods.

(figure 7). Atsumia *et al* (2007) and Jeyadevan *et al* (2009) also reported that superparamagnetic nanoparticles prepared by the co-precipitation method dissipated highest heat to an a.c. magnetic field for hyperthermia. Finally, it is clear to

conclude that the prepared nanomaterials have hyperthermia potentiality synthesized by both methods and hopefully, we are very much interested to use those materials in cancer therapy in future.

## 6. Conclusions

Comparative performances of MNPs prepared by both methods indicate that in respect of heat dissipation capability, saturation values of magnetization and particle size, co-precipitation method is better, whereas in respect of particle shape and absorbance (reflectance), the hydrothermal method is better. Precisely, we can draw a conclusion that MNPs synthesized by the co-precipitation method is better suited for hyperthermia than that by the hydrothermal method. But studies on a.c. magnetic field induced hyperthermia for carcinoma cells are our next step.

## Acknowledgements

The present work was partly supported by Grant-in-Aid for Scientific Research (B) (No.19360367) and Challenging

Exploratory Research (No. 23655204) from Japan Society for the Promotion of Science (JSPS) and Grant-in-Aid for JSPS Fellows (No. 2200083).

## References

- Anselm O 2008 *Synthesis and characterization of tannic acid functionalized magnetic nanoparticles*, in *ACS symposium series 996*, (eds) R Nagarajan and T A Hatton (Washington DC: American Chemical Society) pp 90–107
- Atsumia T, Jeyadevan B, Satob Y and Tohji K 2007 *J. Magn. Magn. Mater.* **310** 2841
- Bate G 1975 in *Magnetic oxides part 2* (ed.) D J Craik (New York: John Wiley & Sons) pp 705–707
- Bautista F M, Campelo J M, Luna D, Marinas J M, Quiros R A and Romero A A 2007 *Appl. Catal.* **B70** 611
- Bertorelle F, Wilhelm C, Roger J, Gazeau F, Ménager C and Cabuil V 2003 *Langmuir* **22** 5385
- Caruso F, Spasova M, Susha A, Giersig M and Caruso R A 2001 *Chem. Mater.* **13** 109
- Cornell R M and Schwertmann U 2003 *The iron oxides: structure, properties, reactions, occurrences and uses* (Weinheim: Wiley-VCH) 2nd ed.
- Häfelí U, Schütt W, Teller J and Zborowski M 1997 *Scientific and clinical application of magnetic carriers* (New York: Plenum)
- Hong D, Xiaolin L, Qing P, Xun W, Jinping C and Yadong L 2005 *Angew. Chem.* **117** 2842
- Hyeon T, Lee S S, Park J, Chung Y and Na H B 2001 *J. Am. Chem. Soc.* **123** 12798
- Jeyadevan B, Atsumia T, Suto M, Kasuya R, Satob Y and Tohji K 2009 *Thermal. Med.* **25** 4
- Karunakaran C and Senthilvelan S 2006 *Electrochem. Commun.* **8** 95
- Kim J S, Yoon T J, Kim B G, Park J S, Kim H W, Lee K H, Park S B, Lee J K and Cho M H 2006 *Toxicol. Sci.* **89** 338
- Laurent S, Forge D, Port M, Roch A, Robic C, Elst L V and Muller R N 2008 *Chem. Rev.* **108** 2064
- Li C, Shen Y, Jia M, Sheng S, Adebajo M O and Zhu H 2008 *Catal. Commun.* **9** 355
- Louie A Y, Huber M M, Ahrens E T, Rothbacher U, Moats R, Jacobs R E, Fraser S E and Meade T J 2000 *Nat. Biotechnol.* **18** 321
- Lu An-Hui, Salabas E L and Schüth F 2007 *Angew. Chem. Int. Ed.* **46** 1222
- Neuberger T, Schopf B, Hofmann H, Hofmann M and Rechenberg B V 2005 *J. Magn. Magn. Mater.* **293** 483
- Perez J M, Simeone F J, Tsourkas A, Josephson L and Weissleder R 2004 *NanoLetters* **4** 119
- Perrin-Cocon L A, Marche P N and Villiers C L 2003 *Biochem. J.* **338** 123
- Shi F, Tse M K, Pohl M M, Bruckner A, Zhang S M and Beller M 2007 *Angew. Chem. Int. Ed.* **46** 8866
- Sun S, Zeng H, Robinson D B, Raoux S, Rice P M, Wang S X and Li G 2004 *J. Am. Chem. Soc.* **126** 273
- Tartaj P, Morales M P, Gonzalez-Carreno T, Veintemillas-Verdaguer S and Serna C J 2005 *J. Magn. Magn. Mater.* **290** 28
- Wang Y, Wong J F, Teng X, Lin X Z and Yang H 2003 *Nano. Lett.* **3** 1555
- Woo K, Lee H J, Ahn J P and Park Y S 2003 *Adv. Mater.* **15** 1761
- Xiong Y, Xie Y, Chen S and Li Z 2003 *Chem. Eur. J.* **9** 4991
- Yu A C C, Mizuno M, Sasaki Y, Kondo H and Hiraga H 2002 *Appl. Phys. Lett.* **81** 3768